

Optical measurements of temperature in a quasi-two-dimensional exciton system

M. R. Reshotko, L. D. Shvartsman, and J. E. Golub

Racah Institute of Physics, The Hebrew University of Jerusalem, Jerusalem, Israel

(Received 10 January 1994)

We have used time-resolved photoluminescence spectroscopy to measure the temperature of a gas of quasi-two-dimensional excitons. The exciton gas consists of both spatially direct and spatially indirect excitons in a coupled GaAs/Al_xGa_{1-x}As double-quantum-well system. We show by experiment and modeling that the ratio of the intensities of the recombination radiation constitutes a sensitive, calibrated thermometer for the electron system. The technique is insensitive to inhomogeneous effects such as well-width fluctuations and is feasible at temperatures as low as several K.

Optical techniques for the determination of electron temperatures have been an important part of fundamental and device-oriented semiconductor physics, and are reviewed thoroughly in Ref. 1. In most systems—especially those related to devices—the emphasis is on fast dynamics. Many measurements have been made on the picosecond and subpicosecond time scales, and have emphasized the interaction of hot carriers with optical phonons, and with each other. Optical measurements have made these interactions directly accessible, and have clarified the limits on device applications.

However, much interesting physics happens closer to equilibrium. An example may be taken from a recent series of papers concerning the possibility of a phase transition in a quasi-two-dimensional (2D) exciton system.²⁻⁷ Electron-hole liquid formation in quantum wells⁸ and electron-hole systems in one dimension⁹ also suggest interesting equilibrium phases. We are therefore motivated to develop optical techniques which permit the dynamic determination of carrier temperature for systems closer to equilibrium.

Here, we report on an absolute measurement of sample temperature based on time-resolved photoluminescence (PL) spectroscopy in a double-quantum-well system. We demonstrate that the gross features of the PL spectra are highly sensitive to temperature in a range inaccessible to traditional techniques. Our method relies only on analysis of such features of the spectra as integrated line intensity, rather than detailed line-shape analysis. Thus, the analysis is not sensitive to delicate features such as those resulting from inhomogeneous broadening. Specifically, we show that the ratio of integrated intensities of two spectral lines can be used to determine the temperature of the quasi-2D exciton system between the time it is heated on excitation and the time it comes to equilibrium with the cooled substrate. The ratio of these two lines in spectra collected after the system has reached equilibrium can be used to calibrate a thermometer for the excitonic system.

The sample consists of coupled GaAs/Al_xGa_{1-x}As quantum wells grown by molecular-beam epitaxy, and has been described in detail elsewhere.¹⁰ Briefly, the sample consists of a single pair of GaAs wells, 10 and 15 nm

in width, separated by a barrier of Al_{0.3}Ga_{0.7}As of thickness 3 nm. The coupled wells lie at the center of a 1- μ m-thick layer of intrinsic material in a *p-i-n* diode. The sample was held in a helium vapor optical cryostat and studied at temperatures between 1.4 and 24 K and at electric fields between 0 and 30 kV/cm. The strength of the electric field was calculated using a built in potential of 1.6 V,¹⁰ and was controlled by varying the *p-i-n* diode bias voltage.

A pair of GaAs quantum wells supports both spatially direct and spatially indirect excitons. When excited, the system evolution includes radiative recombination of each of the exciton species, as well as phonon-assisted scattering between the two states. In a time-resolved experiment, the ratio of the spectrally integrated intensities of the two excitonic lines varies after the time of excitation until it reaches a constant value, determined by the equilibrium temperature of the system. The ratio of intensities reflects the temperature of the exciton gas at any given time, and can be used to determine the temperature in the time before the system comes to equilibrium.

The sample was excited by acousto-optically derived pulses at 1.96 eV. The time resolution of the system was determined by measuring the correlation function of a pulse with the gated detector. This function has a full width at half maximum of 60 nsec with exponential wings characterized by a decay time of 30 nsec. The repetition rate of the pulses is low enough at 200 kHz to allow for complete relaxation of the system between pulses. Each pulse carries an energy of 80 pJ, focused to 500 μ m (the size of the sample), creating an exciton density of at most 10¹⁰ cm⁻². The photoluminescence is dispersed by a 1-m single-grating spectrometer and analyzed by a multichannel photon-counting system.

Figure 1 shows an example of photoluminescence spectra taken at two different temperatures. The spectra were integrated over 200 nsec, beginning 100 nsec after excitation—long enough that the ratio of the integrated intensities is constant. It is clear that the ratio of the intensity of the higher-energy line (I_D , the direct exciton) to that of the lower-energy line (I_I , the indirect exciton), has a sensitive temperature dependence. Spectra of this kind can be considered a type of thermometer, since the

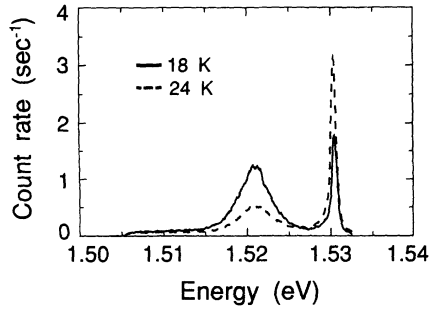


FIG. 1. Photoluminescence spectra integrated from 100 to 300 nsec after excitation for 18 and 24 K.

ratio of the line intensities changes significantly with even small variations in temperature. Such a thermometer can be calibrated by plotting the ratio $r = I_D/I_I$ as a function of the temperature, as we show next.

Figure 2 shows the temperature dependence of the ratio r between 12 and 24 K for three electric fields. These curves calibrate the thermometer mentioned above. The data are well described by a dependence of the form

$$r = r_0 \exp[-\delta/kT], \quad (1)$$

where the parameter δ is calculated from the data to be 7.8, 10.5, and 12.3 meV, and r_0 is found to be 52, 160, and 530 at fields of 19, 24, and 29 kV/cm, respectively. The ratios r_0 derived from Fig. 2 agree well with previous measurements.¹⁰

Figure 3 shows the time evolution of the ratio r . At the lower temperatures (1.4 and 6 K) the decay is simply exponential, while at higher temperatures the ratio approaches a constant value. We interpret this result by saying that for the lower temperatures, the sample does not cool completely over the 200-nsec measurement time. For this reason, the data at lower temperatures were not included in Fig. 2. After such a calibration is made, the temperature can be determined in the system at any time, including in the transient regime, by analyzing the excitonic lines in the spectrum. Thus, if time-resolved data are taken, the temperature of the system at the time each spectrum was collected can be measured absolutely by

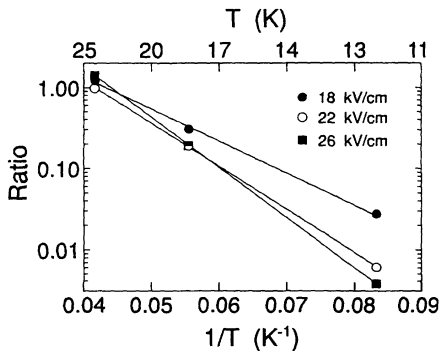


FIG. 2. Temperature dependence of $r = I_D/I_I$ between 12 and 24 K. The lines are best fits according to the parameters given in the text and in Table I.

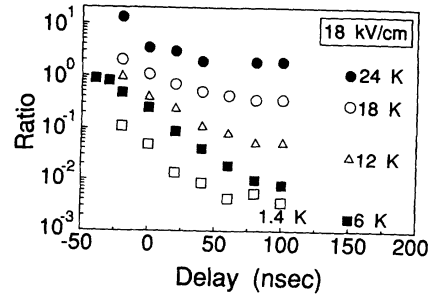


FIG. 3. Time evolution of $r = I_D/I_I$ for various temperatures. The arrows at the right correspond to values of r derived from spectra integrated from 100 to 300 nsec.

comparing it to a spectrum of the type in Fig. 1.

We next discuss these results in terms of the three-level model shown in Fig. 4. The ratio $r = I_D/I_I = \Gamma_{D\rho D}/\Gamma_{I\rho I}$, (I is the intensity, Γ is the recombination rate, ρ is the population density, subscript D represents direct, and subscript I represents indirect), obeys the equation

$$\dot{r} = ar^2 + br + c \quad (2)$$

where the constants are defined as

$$a = \gamma_{D \rightarrow I} \Gamma_I / \Gamma_D, \quad (3)$$

$$b = \Gamma_I - \Gamma_D + \gamma_{I \rightarrow D} - \gamma_{D \rightarrow I}, \quad (4)$$

$$c = \gamma_{I \rightarrow D} \Gamma_D / \Gamma_I. \quad (5)$$

Here, $\gamma_{D \rightarrow I}$ ($\gamma_{I \rightarrow D}$) is the rate for direct to indirect (indirect to direct) conversion via phonon-assisted tunneling. With the assumption of detailed balance

$$\gamma_{I \rightarrow D} = \gamma_{D \rightarrow I} \exp[-\Delta/kT] \quad (6)$$

and the restriction $\Gamma_D \gg \Gamma_I$, the behavior of the ratio at times long after the excitation pulse varies as

$$r(t \rightarrow \infty) = (\Gamma_D / \Gamma_I) [\gamma_{D \rightarrow I} / (\Gamma_D + \gamma_{D \rightarrow I})] \exp[-\Delta/kT]. \quad (7)$$

Here, Δ is the energy splitting between the two exciton states. Equation (7) is just the functional form shown in Fig. 2. We further simplify the equation by assuming that $\gamma_{D \rightarrow I} \gg \Gamma_D$.^{11,12} Equation (7) then reduces to

$$r(t \rightarrow \infty) = (\Gamma_D / \Gamma_I) \exp[-\Delta/kT]. \quad (8)$$

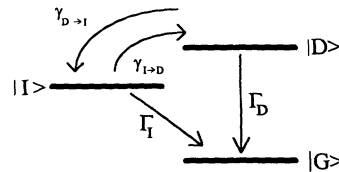


FIG. 4. Three-level model. The rates for spontaneous decay (Γ_D and Γ_I) and for intersystem crossing ($\gamma_{I \rightarrow D}$ and $\gamma_{D \rightarrow I}$) are indicated.

Comparing with the empirical relation Eq. (1), we make the identifications $r_0 = \Gamma_D / \Gamma_I$ and $\delta = \Delta$.

We now quantify the claim that these spectra are highly sensitive to temperature. The maximum observable value of the ratio r is determined by the maximum luminescence rate of the strong line on the one hand, and by the minimum detectable signal on the other. For a slightly modified experimental system and the present sample, this extreme ratio approaches 10^{-8} . This value sets the minimum observable temperature through Eq. (8). For $r_0 \approx 100$ as in the present experiments, the minimum observable temperature is approximately 4 K. Since r_0 varies exponentially with the splitting Δ over a wide range,¹⁰ this ultimate temperature is largely independent of electric field, and can be improved only by recording smaller ratios r . The precision is determined by Eq. (8) to be $dT/T = -(kT/\Delta)dr/r$. In the extreme case of $dr/r \approx 1$, and for $kT/\Delta = k(5 \text{ K})/10 \text{ meV}$, the temperature is determined to 5% precision. In the experiments reported here, the ratio was limited to 10^{-3} , a fact which prevented calibration below $T = 12 \text{ K}$.

We next discuss the three-level model used here. Equation (8) predicts the behavior of Fig. 2 with $\Delta = \delta$ and $r_0 = \Gamma_D / \Gamma_I$. However, comparison of the measured activation energies (δ) with the spectroscopically measured splittings (Δ) shows that δ is consistently smaller by 1–2 meV. To understand this discrepancy, we must consider a more detailed microscopic model, where the energy of each electron is determined not only by quantum confinement, but also by its in-plane motion and by the effects of homogeneous and inhomogeneous broadening. This broadening may be estimated as kT , which in the temperature range in Fig. 2 varies between 1 meV (12 K) and 2 meV (24 K). Thus, the activation energy in Eq. (8) is more accurately estimated as $\delta = \Delta - kT$. These values are summarized in Table I, where it is apparent that the correction brings the model into quantitative agreement with the data. In a detailed, microscopic model, we may expect the rate constants to acquire an electric-field dependence. An extreme example would occur when the splitting Δ is made as large as the optic phonon energy. Still, within these limits, the model offers a framework for quantitative analysis of the data presented here.

Finally, we offer a physical explanation for the behavior of Fig. 3. The light pulse which excites the carriers in the structure also heats the sample significantly, in part because of the large excess energy (nearly 0.5 eV). The temperature relaxation we observe is simply that of

TABLE I. Comparison of measured activation energy (δ) with the spectral energy splitting (Δ). A correction of $kT = 1.5 \text{ meV}$ brings the two energies into good agreement, as described in the text.

Electric field (kV/cm)	δ (meV)	Δ (meV)	$\delta + kT$ (meV)
19	7.85	9.0	9.35
24	10.5	12	12.0
29	12.3	14	13.8

the heated sample cooling to the temperature of the substrate and surrounding helium vapor. To strengthen this hypothesis, we estimated the temperature rise ΔT expected in the sample due to our excitation. The estimation is based on the temperature-dependent (Debye law) heat capacity of GaAs at low temperatures.¹³ This estimated rise was then compared to the temperature rise extracted from the data by analyzing the ratio at $t = 0 \text{ nsec}$ in Fig. 3. The results agree semiquantitatively for the lower temperatures, but do not reflect the observed trend at higher temperatures. This may be due to inadequate time resolution in the present experiment. We further estimated the time for sample cooling by heat diffusion into the substrate. The cooling time was estimated to be much faster than the present time resolution. The apparent decay time of 30 nsec in Fig. 3 is instrumentally limited. Experiments with sources of a different excitation energies and with improved time resolution are necessary to complete picture.

In conclusion, we have demonstrated an optical technique for measuring carrier temperature in a quasi-2D system. Importantly, the technique is calibrated, and does not rely on a detailed line-shape analysis or on a detailed theoretical model. We have discussed the system in terms of a simple three-level model and shown the validity of the model in describing our data in the steady-state limit. We have ascribed the observed dynamic behavior to heat diffusion through the quantum layer, and into the surrounding environment. It is of interest to extend this technique to the regime of nonequilibrium between electrons and phonons. Future work will address this possibility.

We thank D. Romanov for discussions and A. Gabai for technical assistance. This research was supported by the Basic Research Foundation administered by the Israel Academy of Sciences and Humanities.

¹Hot Carriers in Semiconductor Nanostructures, edited by J. Shah (Academic, New York, 1992).

²Yu. E. Lozovik and V. I. Yudson, Zh. Eksp. Teor. Fiz. **71**, 738 (1976) [Sov. Phys. JETP **44**, 389 (1976)].

³S. I. Shevchenko, Fiz. Nizkik Temp. **2**, 505 (1976) [Sov. J. Low Temp. Phys. **2**, 251 (1976)].

⁴T. Fukazawa, S. S. Kano, T. K. Gustafson, and T. Ogawa, Surf. Sci. **228**, 482 (1990).

⁵T. Fukazawa, E. E. Mendez, and J. M. Hong, Phys. Rev. Lett.

64, 3066 (1990)

⁶J. Kash, M. Zachau, E. E. Mendez, J. M. Hong, and T. Fukazawa, Phys. Rev. Lett. **66**, 2247 (1991).

⁷Z. Gedik and S. Ciraci, J. Phys. Condens. Matter **2**, 8985 (1990).

⁸H. Kalt, R. Notzel, K. Ploog, and H. Giessen, Phys. Status Solidi B **173**, 389 (1992).

⁹N. Nagaosa and T. Ogawa, Solid State Commun. **88**, 295 (1993).

¹⁰J. E. Golub, K. Kash, J. P. Harbison, and L. T. Florez, *Phys. Rev. B* **41**, 8564 (1990).

¹¹D. Y. Oberli, J. Shah, T. C. Damen, C. W. Tu, T. Y. Chang, D. A. B. Miller, J. E. Henry, R. F. Kopf, N. Sauer, and A. E.

DiGiovanni, *Phys. Rev. B* **40**, 3028 (1989).

¹²M. Nido, M. G. W. Alexander, W. W. Ruhle, T. Schweizer, and K. Kohler, *Appl. Phys. Lett.* **56**, 355 (1990).

¹³J. S. Blakemore, *J. Appl. Phys.* **53**, R123 (1982).